

**Fatigue Crack Propagation Behavior in Butt Weldment of
SA106 Gr.C Main Steam Pipe Steel**

Eung Seon Kim, Chan Su Jang and In Sup Kim
Korea Advanced Institute of Science and Technology

Abstract

The fatigue crack propagation behavior in SA106 Gr.C main steam pipe weld joint was investigated in air environment. Crack growth rate tests were conducted on base metal and weld metal at load ratio of 0.1 and 0.5 and at frequency of 10Hz. The fatigue crack growth rates of the base metal and the weld metal were above the ASME reference line and the fatigue crack propagation rate of the weld metal was higher than those of the base metal. Fatigue crack growth rate increased with increasing the load ratio and the effect of the load ratio was more significant in the weld metal. The post weld heat treatment increased the fatigue crack growth rates of the base metal by reducing compressive residual stress and decreased those of the weld metal by reducing weld defects.

I. Introduction

The SA106 Gr.C is a C-Mn low alloy steel widely used as a main steam pipe for nuclear power plants. The lifetime of pipings is largely dependent upon fatigue crack propagation behavior of the material used under the actual operating conditions of a nuclear power plant [1, 2]. Fatigue cracks often originate at welded joints and fatigue crack growth rate in welded joints may be influenced by microstructure, mechanical heterogeneity and residual stress [3]. To remove the residual stress, post weld heat treatment is performed by local heating a circumferential band around weld joint. In this process, base metal can be affected by the post weld heat treatment. Since welding is employed as the main method of joining the pipe, knowledge of the crack growth behavior in weldment is usually necessary. However, there is only limited works on the fatigue behavior of main steam pipe.

The objective of this study is to understand the effect of load ratio and post weld heat treatment on the fatigue crack growth rate of SA106 Gr.C main steam pipe weld joints in air environment.

II. Experimental Procedures

The base metal used in the present study was a 667mm O.D. and 28.7mm thickness SA106 Gr.C low alloy steel supplied by the Korean Heavy Industries & Construction Co., Ltd. The

weld joint was produced by a gas tungsten arc welding process (GTAW) with a AWS Class ER70S-6 wire, ϕ 2.4mm. The chemical compositions and the mechanical properties are given in Tables I and II, respectively. The welding conditions are summarized in Table III. The welding line is along the circumferential direction of the pipe. Both materials were stress-relieved for 1hr at 600°C to account for the effect of post weld heat treatment. The microstructures of the base metal and the weld metal were examined with optical microscope.

Standard compact tension specimens of 51mm width and 12.5mm thickness were employed for fatigue crack growth tests and the orientation of crack was the circumferential direction of the pipe.

Fatigue crack growth tests were conducted at room temperature at the load ratios of 0.1 and 0.5 on a INSTRON closed-loop servo-hydraulic testing machine. A sinusoidal wave form was used at frequency of 10Hz. Crack length, a , was estimated from specimen compliance with clip-on gage. compliance measurements were based on the upper linear portion of the load vs. COD (crack opening displacement) traces and were stored, with the cycle counts, at crack length intervals of 0.2mm. Applied stress intensity was calculated using the expression in ASTM E647-94 for CT specimens. Crack closure levels were determined statistically using the upper tangent point, and nonsubjectively by measuring the 2% deviation from the upper portion of load vs. COD traces [4]. The fracture surfaces of the tested specimens were examined with a scanning electron microscope (SEM).

III. Results and Discussion

III.1 Microstructure and Tensile Properties

The optical micrographs of the base metal and the weld metal are shown in Fig. 1. The base metal is a ferrite-pearlite banding structure. It is caused by the interdendritic segregation of Mn during solidification [5]. The equiaxed fine ferrites are the main constituents of the weld metal. The average ferrite grain size of the base metal is slightly larger than that of the weld metal. As shown in Table. II, the yield strength and ultimate strength for the weld metal are larger than those for the base metal. This is believed to be because of the smaller grain size of the weld metal. Microstructural differences due to the post weld heat treatment were not discernible by optical microscopy but the tensile strength of the weld metal decreased after the post weld heat treatment.

III.2 Fatigue Crack Growth Behavior

The fatigue crack propagation rates da/dN with stress intensity factor range ΔK for the base metal and the weld metal are shown in Fig. 2 and Fig. 3, respectively. The reference line for the crack propagation rates in air given in ASME Boiler and Pressure Vessel Code, Section XI is also included for comparison [6]. It can be seen that the crack propagation rates in air determined in the present study are above the ASME reference line and the fatigue

crack propagation rates of the weld metal are higher than those of the base metal in the ΔK range examined.

In the case of the base metal, increasing load ratio increases the crack propagation rates with decreasing ΔK levels. But the load ratio effect is reduced after the post weld heat treatment. The effects of load ratio on fatigue crack propagation have been mainly treated in the near threshold region, while it has been neglected in the Paris' linear region [7]. However the influence of load ratio on the crack propagation rates of the weld metal was found to be even pronounced in Paris' region.

The sensitivity of fatigue crack propagation to load ratio is caused by crack closure which is crack wake surface contact during the unloading of a fatigue cycle. Crack closure reduces the applied stress intensity range, ΔK , to an effective value defined as $\Delta K_{eff} = K_{max} - K_{cl}$ ($>K_{min}$). Several crack closure mechanisms have been report such as roughness induced crack closure, oxide induced crack closure, plasticity induced crack closure, etc [8].

To clarify the load ratio effect, the values of the K_{cl}/K_{max} as a function of ΔK were measured and given in Fig. 4. It can be seen that the crack closure were higher at the load ratio 0.1 than at the load ratio of 0.5 in low ΔK region but as crack grew, the crack closure maintained constant level. In low ΔK region (near-threshold region), crack closures are induced by the roughness of the fracture surface and oxide filling due to fretting. Considering that the microstructure of the base metal after the post weld heat treatment was not altered, the crack closure of the base metal at the load ratio of 0.1 is thought to be caused by the compressive residual stress induced during manufacturing process. It is well known that the compressive residual stress affects on the crack tip stress field and decreases effective stress intensity factor range [9].

$$\Delta K_{eff} = K_{eff}^{max} - K_{eff}^{min} = (K_{nom}^{max} + K_{res}) - K_{eff}^{min}$$

where $K_{eff}^{min} > 0$ and $> K_{nom}^{min} + K_{res}$

So the increase in the crack growth rate and the decrease in the crack closure level of the base metal at the load ratio of 0.1 can be explained with the elimination of the compressive residual stress after the post weld heat treatment.

As shown in Fig. 4 the crack closure of the weld metal was not influenced by the post weld heat treatment and load ratio in the Paris' region. Therefore the effects of the load ratio and post weld heat treatment on the fatigue crack growth behavior can not be explained with the crack closure.

Fig. 5 shows the fracture surfaces of the specimen tested, where the crack propagation rates were in the Paris' region. The fracture surface of the base metal shows striations whereas the fatigue fracture mode of the weld metal is intergranular mode. This mean that certain factors affect on the intrinsic fatigue crack growth rate of the weld metal. Segregations, inclusions and porosities during multi-pass welding acts as crack initiation sites and stress concentrations [10], so these can accelerate the fatigue crack propagation rates of the weld metal.

IV. Conclusions

The fatigue crack propagation behavior of ASME SA106 Gr.C main steam pipe weld joint in air environment has been investigated. The results obtained are follows.

1. The fatigue crack propagation rates of SA106 Gr.C weld joint were found to be above the reference line given in ASME Boiler and Pressure vessel Code Sec. XI.
2. The fatigue crack propagation rates of the weld metal are higher than those of the base metal in the ΔK range examined.
3. Increasing load ratio increased the fatigue crack growth rates. The effect of the load ratio was more pronounced in the weld metal.
4. Post weld heat treatment decreased the compressive residual stress of the base metal which was introduced during manufacturing process and the weld defects.

Acknowledgement

This work was financially supported by Korea Science and Engineering Foundation through the Center for Advanced Reactor Research.

References

- [1] George J. Theus and John R. Weeks, Environmental Degradation of materials in Nuclear Power System-Water Reactor (1988)
- [2] A. Saxena and P.K. Liaw, Eng. Frac. Mech., 45(1993)759
- [3] H.O. Fuchs and R.I. Stephens, Metal Fatigue in Engineering (1980)262
- [4] J.K. Donald, Mechanics of Fatigue Crack Closure, ASTM STP 982(1988)222
- [5] William C. Leslie, The Physical Metallurgy of Steels (1982)172
- [6] ASME Boiler and Pressure Vessel Code, Sec. III, Div, 1, App. A, ASME, New York (1989)
- [7] D. Taylor, Fatigue Thresholds, Butterworth (1989)
- [8] A.K. Vasudeven, K. Sadanada and N. Louat, Mat. Sci. & Eng. A188(1994)
- [9] L. Bertini, Theoretical and Applied Fracture Mechanics, 16(1991)135
- [10] J.P. Sandifer and G.E. Bowie, Fatigue Testing of Weldments, ASTM STP 648(1978)185

Table I. Chemical compositions of the SA106 Gr.C steel and the filler metal (in wt%)

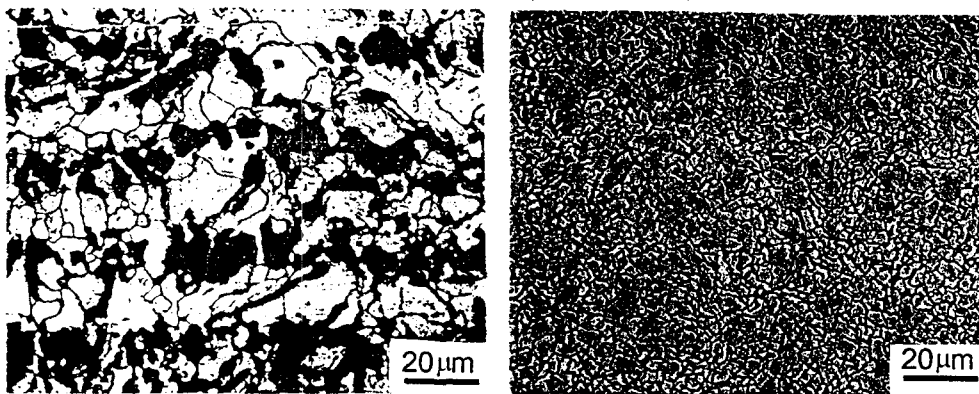
Element	C	Mn	P	S	Si	Ni	Cr	Mo	V	Al	Cu
SA106 Gr.C	0.19	1.22	0.009	0.007	0.27	0.11	0.05	0.03	0.004	0.029	0.13
Filler metal	0.08	1.55			0.85						

Table II. Tensile properties of the base metal and the weld metal

Stress-relief	No		Yes	
	Base metal	Weld metal	Base metal	Weld metal
Y.S.(MPa)	349	555	335	541
U.T.S.(MPa)	548	650	556	696

Table III. Welding conditions of GTAW

Preheat temperature	Min.	120 °C
Interpass temperature	Max.	250 °C
Ampare range		100 - 150 A
Voltage range		10 - 18 V
Travel Speed		10 - 15cm/min



(a)

(b)

Fig. I. Optical micrographs of (a) the SA106 Gr.C and of (b) the weld metal

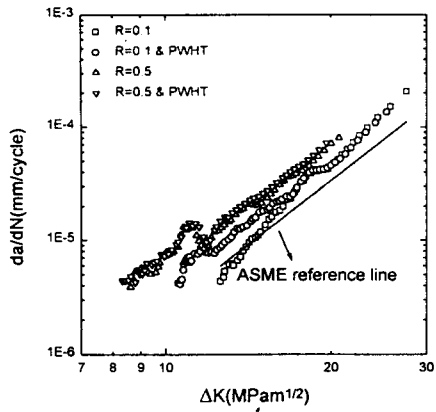


Fig. 2. Fatigue crack propagation rates for the base metal

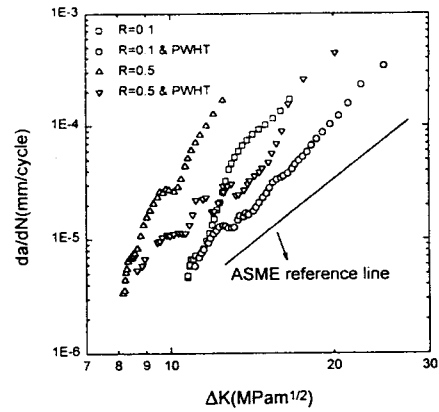


Fig. 3. Fatigue crack propagation rates for the weld metal

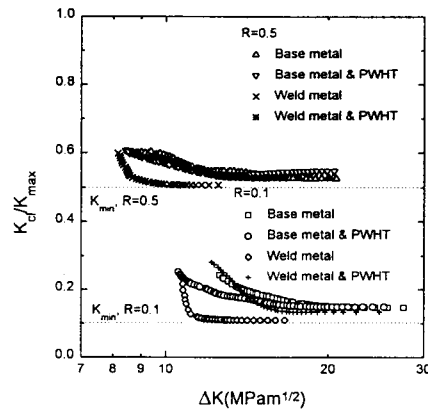
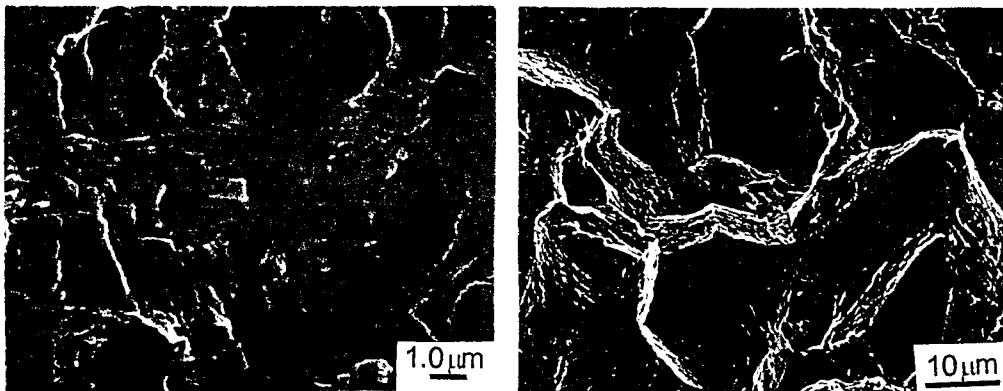


Fig. 4. Variation of the K_{cl}/K_{min} at load ratio of $R=0.1$ and 0.5



(a)

(b)

Fig. 5. Scanning electron micrographs of (a) the base metal and (b) the weld metal in the Paris' linea region